Optical spectrum and Jahn-Teller splitting of Cu^{2+} sites in K_2CuF_4 based on *ab initio* studies of $(CuF_6)^{4-}$ clusters

Sergei Yu. Shashkin* and William A. Goddard III
Arthur Amos Noyes Laboratory of Chemical Physics, California Institute of Technology, Pasadena, California 91125
(Received 26 July 1985)

Using a $(CuF_6)^{4-}$ cluster plus up to 30 counterions to model the Cu^{2+} site in K_2CuF_4, we carried out Hartree-Fock and configuration-interaction (CI) calculations for all five states corresponding to the d^9 configuration of Cu^{2+}. We find that electron correlation CI leads to an increased importance of charge transfer states and a 20% increase in ligand field separations. The CI calculation gives good agreement with experimental ligand field spectra and confirms one of the two previous assignments. We also examined various distortions of the $(CuF_6)^{4-}$ cluster and extracted the Jahn-Teller (JT) coupling constants. These results support a previous analysis (based on semiempirical calculations) of the cooperative Jahn-Teller ordering observed in $KCuF_3$ and K_2CuF_4; however, the present results find that this ordering distortion is dominated by the anharmonic term of the potential energy associated with fluorine e_g displacements (second-order JT interactions account only for 10% of the effect).

I. INTRODUCTION

The K_2CuF_4 crystal possesses pseudo-octahedral $(CuF_6)^{4-}$ complexes, but distortions lead to a complicated crystal structure with peculiar orbital and magnetic ordering.[1] A number of crystallographic[2] and spectroscopic studies[3-5] have been carried out; however, there are significant uncertainties in the explanation. For a perfect octahedral geometry, the d^9 configuration of Cu^{2+} is expected to split into a ^2E_g ground state (d-hole orbitals pointing toward F^- ligands) and a $^2T_{2g}$ excited state. However, from the Jahn-Teller (JT) theorem, one expects the local symmetry to distort so as to split the ^2E_g state, forming a spatially nondegenerate ground state. Indeed, the complicated crystal structure has been explained[6,7] as due to a cooperative JT distortion at each Cu atom. Which type of superlattice ordering is stabilized in K_2CuF_4 (and in $KCuF_3$) depends critically on the values of the JT coupling (JTC) constants for Cu^{2+}, but only some of these constants could be evaluated using the previous semiempirical approach.[7] Consequently, we undertook *ab initio* studies to provide a more quantitative test of the origins for these distortions.

The optical-absorption spectrum of the crystal provides essential information concerning the electronic structure at the distorted Cu^{2+} sites, and therefore, correct interpretation of the K_2CuF_4 optical spectrum is of importance. The nearest fluorine neighbors form an elongated octahedron[2] with D_{4h} symmetry, but the exact site symmetry at the copper atoms in K_2CuF_4 is D_2. Three absorption bands are observed experimentally[3,4] with the maxima at 8400, 9400, and 12 200 cm^{-1} (the first moments are at 7940, 9520, and 12 300 cm^{-1}). Two different interpretations of these results have been given in the literature.[1,3-5] Semiempirical calculations of the energy spectrum and JTC constants of the $(CuF_6)^{4-}$ cluster[8] have strongly supported the assignment of the K_2CuF_4 absorption bands as transitions from $^2B_{1g}$ to $^2A_{1g}$, $^2B_{2g}$, and ^2E_g (presuming D_{4h} local symmetry), as suggested in Refs. 1 and 4. However, good quantitative agreement between the calculated and experimental optical spectra was not obtained.[8]

The previous semiempirical calculations on $(CuF_6)^{4-}$ were based on molecular-orbital (MO) methods and did not include the effects of electron correlation. Since recent *ab initio* configuration-interaction (CI) calculations of the CuF_2 molecule[9-11] have shown that electron correlation leads to a 20% increase in ligand field splittings, we examined the effects of electron correlation on cluster models of the Cu^{2+} site in K_2CuF_4. The present paper reports *ab initio* (nonempirical) Hartree-Fock (HF) and CI calculations on the $(CuF_6)^{4-}$ cluster supplemented with various numbers of point charges. We used these calculations to interpret the optical absorption of K_2CuF_4 and the JTC constants for tetragonal and totally symmetric distortions of $(CuF_6)^{4-}$.

II. COMPUTATIONAL DETAILS

A. Cluster models

The crystal structure of K_2CuF_4 has space group D_{2d}^{10} ($I\bar{4}c2$); the tetragonal unit cell contains eight formula units; and the copper ions occupy $4a$ and $4d$ positions, both with D_2 symmetry.[2] Each copper ion is surrounded by an elongated fluorine octahedron (D_{4h} symmetry) with four F^- at 1.92 Å and two F^- at 2.22 Å. The next neighbors for each Cu^{2+} are eight potassium ions, lowering the copper site symmetry to D_{2h}. Considering only ions situated inside the sphere of radius 5 Å around each Cu^{2+} ion (more distant ions were found negligible in the cluster-model calculations of $KNiF_3$) (Ref. 12) leads to exactly the same D_{2h} symmetry environment for both $4a$ and $4d$ positions. We have investigated the crystal environment influence on the $(CuF_6)^{4-}$ energy spectrum by carrying out fully-self-consistent HF calculations on the following:

(a) the free $(CuF_6)^{4-}$ cluster;

(b) the $(CuF_6)^{4-}$ cluster supplemented with eight point charges placed at the potassium positions nearest to the Cu^{2+} (the point charges on each K were chosen as $+\frac{1}{2}$ to retain electroneutrality of the whole system) [this model is denoted as $\{(CuF_6)^{4-}+8$ point charges$\}$]; and

(c) the $(CuF_6)^{4-}$ cluster supplemented with 30 point charges situated inside a sphere of radius 5 Å around the copper ion (charges of $+1$ and $+2$ were attributed to the internal K and Cu ions, respectively, and charges of -0.875 were attributed to 16 boundary fluorines to retain charge neutrality) [this model is denoted as $\{(CuF_6)^{4-}+30$ point charges$\}$].

For the D_{4h} distortion of the F neighbors (elongation along the z axis), the cubic ^2E_g ground state of d^9 configuration splits into levels of $^2B_{1g}$ and $^2A_{1g}$ symmetry, with the states corresponding to x^2-y^2 ($^2B_{1g}$, lower level) and z^2 ($^2A_{1g}$, upper level) character. The excited $^2T_{2g}$ state splits into $^2B_{2g}$ (lower) and ^2E_g (upper) levels corresponding to xy and xz,yz states, respectively. The distant point charges included in the cluster lead to D_{2h} symmetry, and our discussions below will use the irreducible representations appropriate for D_{2h}. The symmetry reduction $D_{4h}\rightarrow D_{2h}$ causes a small mixing of the x^2-y^2 and z^2 states (both are ^2A_g for D_{2h} symmetry) and full splitting of the $^2T_{2g}$ state into $^2B_{1g}$ (xy), $^2B_{2g}$ (xz), and $^2B_{3g}$ (yz) states.

B. Basis set

Most of our calculations were performed with the Cu^{2+} and F^- Gaussian valence double-zeta basis sets developed in Ref. 11, but we also calculated the free $(CuF_6)^{4-}$ cluster using the valence double-ζ basis sets contracted for the neutral Cu and F atoms (with diffuse s and p exponents eliminated from the F basis).

C. CI calculations

We utilized some of the simplifications in the CI calculations for $\{(CuF_6)^{4-}+30$ point charges$\}$ that were developed in Ref. 11 for CuF_2. The sequence was as follows.

(i) We carried out separate, fully-self-consistent HF calculations on the dominant d-shell state of each symmetry, $^2B_{1g}$, $^2B_{2g}$, and $^2B_{3g}$, and on the ground and excited states of ^2A_g for $\{(CuF_6)^{4-}+30$ point charges$\}$. We performed self-consistent HF calculations for the excited ^2A_g state by starting with orbitals obtained in a preliminary HF calculation that neglected the off-diagonal Hamiltonian matrix elements between the (x^2-y^2)-like and z^2-like orbitals (i.e., the D_{4h} symmetry of all orbitals was retained but the influence of the low-symmetry crystal field on the one-electron energies of these orbitals was taken into account). We then iterated on the excited state using the upper root for the rotations between occupied a_g orbitals and using overlap to select the occupied eigenfunctions from the OCBSE Fock matrices.[13] In the CI calculation for the ^2A_g states, we used the valence space of orbitals obtained in an HF calculation on the ground ^2A_g state but allowed the doubly occupied orbitals to be mixed for an optimal description of the singly occupied orbital of the excited ^2A_g state. Thus we projected the open-shell z^2-like orbital *optimized for the excited* ^2A_g *state* onto the 13 doubly occupied a_g orbitals optimized for the ground ^2A_g state to obtain a localized z^2-like orbital. This z^2-like projection and the initial (x^2-y^2)-like orbital optimized for the ^2A_g ground state are automatically orthogonal to each other and give a good description of the d-like orbitals in the CI calculation for ^2A_g states. The remaining 12 doubly occupied a_g orbitals were obtained from the self-consistent a_g orbitals of the ^2A_g ground state by Schmidt orthogonalization to this z^2-like projection. The procedure described is a unitary transformation within the doubly occupied orbitals of the ground ^2A_g state, and hence does not change the HF energy of this state.

(ii) In each case, the self-consistent corelike molecular orbitals (F $1s$ and $2s$, Cu $1s$, $2s$, $2p$, $3s$, and $3p$) were considered as a fixed core for the CI calculation (the validity of ignoring the excitations from the valence F $2s$—like orbitals was established in the CI calculations of CuF_2).[11] This leaves a total of 23 occupied orbitals (five a_g, three b_{1g}, three b_{2g}, three b_{3g}, three b_{1u}, three b_{2u}, and three b_{3u}).

(iii) In accordance with the conclusions of Ref. 11 about the particularly important role of charge transfer (CT) in the CI for ligand field splittings, we considered excitations from both the dominant (d-shell) and CT configurations. For example, for $^2B_{1g}$ (xy), the dominant configuration can be visualized as in Fig. 1 (d^9-like state), where the Cu d_{xy} orbital is singly occupied and only those F orbitals that are π_x- or π_y-like with respect to the appropriate Cu—F bonds are shown. Important CT terms of $^2B_{1g}$ symmetry can be thought of as combinations of valence-bond configurations such as in Fig. 1 [charge transfer (d^{10}) state]. For D_{2h} symmetry, the $\{(CuF_6)^{4-}+30$ point charges$\}$ cluster has three CT states of ^2A_g symmetry and two CT states each of $^2B_{1g}$, $^2B_{2g}$, and $^2B_{3g}$ symmetry. Therefore, for the ^2A_g state we allowed CI excitations from five reference configurations (two d-shell states plus three CT states) and solved for the two lowest roots

TABLE I. The calculated energy spectrum of $(CuF_6)^{4-}$ clusters for a_{1g} distortions (the reference energy is -2232.0 a.u.).

$(1/\sqrt{6})Q_a$ (Å)	$E(^2E_g)$ (a.u.)		$E(^2T_{2g})$ (a.u.)	
	HF	CI	HF	CI
−0.03	−0.627 515	−0.637 036	−0.603 671	−0.607 156
0.00	−0.641 819	−0.650 884	−0.620 127	−0.623 440
0.03	−0.653 740	−0.662 387	−0.633 982	−0.637 144

TABLE II. The calculated energy spectrum of $(CuF_6)^{4-}$ cluster for $e_g(Q_\theta)$ distortions (the reference energy is -2232.0 a.u.).

$(1/\sqrt{6})Q_\theta$ (Å)	$E(^2A_{1g})$ (a.u.)		$E(^2B_{1g})$ (a.u.)		$E(^2B_{2g})$ (a.u.)		$E(^2E_g)$ (a.u.)	
	HF	CI	HF	CI	HF	CI	HF	CI
−0.06	−0.643 951	−0.654 367	−0.629 840	−0.637 739	−0.612 212	−0.615 173	−0.616 089	−0.619 841
−0.03	−0.644 196	−0.653 920	−0.637 208	−0.645 660	−0.617 651	−0.620 773	−0.619 529	−0.622 999
0.03	−0.637 384	−0.645 832	−0.644 270	−0.654 001	−0.620 204	−0.623 735	−0.618 434	−0.621 692
0.06	−0.631 120	−0.639 007	−0.644 836	−0.655 278	−0.618 138	−0.621 914	−0.614 683	−0.617 977
0.05/3[a]	−0.633 447	−0.642 355	−0.637 417	−0.647 054	−0.613 454	−0.616 964	−0.612 440	−0.615 783

[a]This geometry corresponds to $R_{Cu\text{-}F}=2.00$ Å (four) and $R_{Cu\text{-}F}=2.05$ Å (two), and therefore there is $Q_a=-(0.08/\sqrt{6})$ Å except for $Q_\theta=(0.1/\sqrt{3})$ Å.

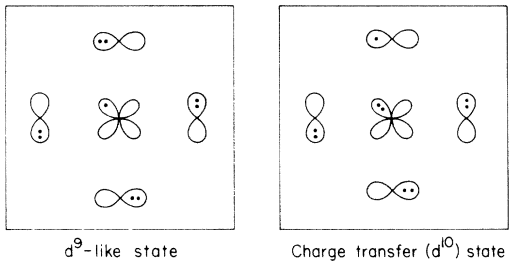

FIG. 1. Valence-bond representation of d^9-like and charge transfer states of $^2B_{1g}$ (xy) symmetry.

of the CI matrix. For each ^{2}B state, we allowed excitations from three reference configurations (one d-shell state plus two CT states) and solved for one lowest root of the CI matrix.

(iv) In Ref. 11, we showed that the total number of virtual orbitals in the CI could be reduced by solving self-consistently for the orbitals of the CT state. For example, for $^2B_{1g}$ symmetry, we start with the fully-self-consistent ground state (d_{xy}-like hole in a $3b_{1g}$ orbital) and fix all core orbitals and the $1b_{1g}$,$2b_{1g}$ CT orbitals. We then construct the two CT configurations with the electron transferred to $3b_{1g}$ from $1b_{1g}$ or $2b_{1g}$. Constructing Fock Hamiltonians corresponding to the average energy of these two CT states, we solve for the remaining 21 valence orbitals self-consistently. We then fix these valence orbitals and resolve for the $1b_{1g}$,$2b_{1g}$ CT orbitals. The net result is 23 valence orbitals optimized for describing CT. We then Schmidt-orthogonalize these 23 to the corresponding 23 valence orbitals from the ground $^2B_{1g}$ state to obtain a 46-orbital space equally suitable for describing both ground and CT $^2B_{1g}$ states. This *modified virtual space* (MVS) allows us to construct CI wave functions using 46 rather than 60 orbitals (21 orbitals are included into the core), considerably simplifying the CI calculation.

The above simplifications lead to a considerable reduction in the number of orbitals for the CI (from 81 to 46); however, allowing all *single and double excitations* from the d shell and the CT configurations still yields rather large CI wave functions (171 843 spin eigenfunctions for ^2A_g and 114 411 spin eigenfunctions for the ^{2}B states). Consequently, for these studies of $\{(CuF_6)^{4-}+30$ point charges$\}$, we allowed all *single excitations* from the d shell and CT configurations. This leads to very simple CI wave functions with dimensions of 670 and 450 for the ^2A_g and ^2B states, respectively.

In addition to the above studies, we also tested the approach of using *average-of-configuration* (AC) orbitals.[11] In the AC approach we solve for an average d^9 configuration having 1.8 electrons in each of the five d-like orbitals. Similarly, for the CT wave function we carry out the AC HF calculation with ten electrons in the d shell and one hole distributed over all nine CT orbitals.

D. Spin-orbit coupling

The spin-orbit interaction effects were evaluated approximately by considering only one-center spin-orbit interactions using $\zeta_{3d}=830$ cm^{-1}. Thus the $(CuF_6)^{4-}$

ligand field states were treated as if there was a hole localized in the copper d shell but with energies as obtained in the CI calculations.

E. Jahn-Teller coupling constants

The JTC and harmonic force constants of the free $(CuF_6)^{4-}$ cluster were evaluated from the series of the HF and CI calculations using the AC approximation. These calculations were carried out for a number of octahedral and tetragonally distorted configurations of $(CuF_6)^{4-}$, as indicated in Tables I and II.

III. RESULTS

A. Ligand field splitting in K_2CuF_4

Table III summarizes the results of the HF and CI calculations on various clusters modeling the K_2CuF_4 crystal. Comparison of the first two rows shows that replacement of the basis sets optimized for the neutral atoms by the basis sets optimized for Cu^{2+} and F^- increases the π energy gap [$^2B_{2g}(xz)$,$^2B_{3g}(yz)$ relative to the $^2B_{1g}(xy)$ state] by 19% while the σ energy gap (between the ground and excited ^2A_g states) increases only by 1%. Thus the π-type states are somewhat more sensitive to the basis set (neutral versus ionic) than are the σ-type states.

Comparing rows 2, 3, and 4, we see that supplementing the $(CuF_6)^{4-}$ cluster with point charges modeling the K_2CuF_4 crystal environment results in small increases for both the σ and π energy gaps (about 10% and 2%, respectively). Note that the point-charge contributions to the separation between $^2B_{2g}$ and $^2B_{3g}$ levels (degenerate in D_{4h} symmetry) from the nearest eight ions (row 3) and from the next 22 ions (row 4) partially compensate each other, leading to a net energy-gap value of only 91 cm^{-1}. These results confirm the adequacy of using the simple nearest-neighbor cluster model for ionic crystals (as previously established for $KNiF_3$ by Ref. 12 and references therein).

Including correlation effects leads to a marked improvement in the agreement between the calculated d-d transition energies for $\{(CuF_6)^{4-}$ + 30 point charges$\}$ and the experimental K_2CuF_4 absorption spectrum (e.g., compare rows 4 and 6 in Table III). Thus the CI leads to an increase in d-d excitation energies by about 20%. The important role of the CT configurations found in Ref. 11 can be ascertained by comparing the results of CI calculations using only the d^9-like dominant configurations as reference states (row 5) with comparative calculations using both the d shell and the CT configurations as reference states (row 6).

Including one-center spin-orbit corrections (compare rows 6 and 7) gives a considerably increased separation (from 90 to 783 cm^{-1}) of the two upper levels (xz and yz). This is easy to understand. Neglecting the spin-orbit interaction of xz and yx states with xy, z^2, and (x^2-y^2) states (which are stabilized by ligand field interactions), one obtains two Kramers doublets with orbital wave functions $(yz)\pm i(xz)$ and an energy separation of $\zeta_{3d}=830$ cm^{-1}. Consequently, the spin-orbit interaction leads to a general increase in the splitting of the levels arising from

TABLE III. The K_2CuF_4 optical-absorption spectrum based on calculations for various $\{(CuF_6)^{4-}$ + point charges$\}$ cluster models.

Method	Number of point charges	Comments	^2A_g ground-state energy (a.u.)	Energies of d-d excitations (cm^{-1}) ^2A_g ($\sim z^2$)	$^2B_{1g}$ (xy)	$^2B_{2g}$ (xz)	$^2B_{3g}$ (yz)
HF	0	neutral basis[a]	−2232.424 258	5131	7108	8259	8259
HF	0		−2232.639 008	5170	6986	8405	8405
HF	8		−2285.037 050	5314	7333	8745	8612
HF	30		−2307.842 678	5778	7243	8650	8741
CI	30	no CT[b]	−2307.846 425	6318	7827	9270	9362
CI	30		−2307.853 845	7142	8892	10 499	10 589
CI	30	spin orbit[c]	−2307.854 324[d]	6993[d]	8796[d]	10 537[d]	11 320[d]
HF	30	AC[e]	−2307.841 288	5880	7190	8595	8686
CI	30	AC[e]	−2307.853 818	7052	8920	10 505	10 593
CI	30	AC,[e] spin orbit[c]	−2307.854 292[d]	6908[d]	8820[d]	10 545[d]	11 318[d]
Expt.[f]				7940	9520	12 300[g]	12 300[g]

[a]Gaussian basis sets obtained for neutral F and Cu atoms are used instead of the basis sets optimized for F^- and Cu^{2+}.
[b]Excitations from the CT configurations are not taken into account in the CI.
[c]One-center spin-orbit corrections are taken into account.
[d]This is the energy of the Kramers doublet state; the wave function is a linear combination of all five d-like states.
[e]The average-of-configuration calculation (AC approximation).
[f] Reference 4.
[g]The two upper states are not resolved experimentally.

the $^2T_{2g}$ state of octahedral symmetry. The result is a total calculated separation of 2524 cm^{-1} for the $^2T_{2g}$ band, giving a possible explanation for the rather large difference of 2780 cm^{-1} between the B_1 [$^2A_g \rightarrow {}^2B_{2g}(xz)$, $^2B_{3g}(yz)$] and B_2 [$^2A_g \rightarrow {}^2B_{1g}(xy)$] absorption bands observed experimentally.[3,4] The splitting of the broad (2740 cm^{-1} half-width) B_1 band has not been resolved experimentally.

The utility of the AC approximation was previously discussed in connection with HF and CI calculations on CuF_2.[11] We see from Table III that this approach yields good results for modeling K_2CuF_4 while considerably simplifying the calculations. The AC approach was used in the HF and CI calculations for the JTC constants of $(CuF_6)^{4-}$.

B. Jahn-Teller coupling constants

We considered the tetragonal e_g and totally symmetric a_{1g} distortions of the free octahedral $(CuF_6)^{4-}$ cluster starting with $R_{Cu\text{-}F}=2.03$ Å (the average Cu-F distance for a number of ionic crystals containing copper).[2] The coordinates of the e_g displacements are designated by Q_θ and Q_ϵ and those of the a_{1g} displacements by Q_a. These symmetrized coordinates are represented in terms of the Cartesian coordinates of separate fluorine ion displacements, as in the Appendix. The adiabatic potential matrices ($\underline{W}$) for the ground ^2E_g and excited $^2T_{2g}$ states of $(CuF_6)^{4-}$ can be expanded in terms of the a_{1g} and e_g displacements as follows:

$$\underline{W}(^2E_g)=[\tfrac{1}{2}K_aQ_a^2+\tfrac{1}{2}K_e(Q_\theta^2+Q_\epsilon^2)+V_aQ_a+A(Q_\theta^3-3Q_\theta Q_\epsilon^2)]\underline{1}_0-[(V_e+PQ_a)Q_\theta+N_e(Q_\epsilon^2-Q_\theta^2)]\underline{\sigma}_z$$
$$+[(V_e+PQ_a)Q_\epsilon+2N_eQ_\epsilon Q_\theta]\underline{\sigma}_x\ , \tag{1}$$

$$\underline{W}(^2T_{2g})=[\tfrac{1}{2}K_aQ_a^2+\tfrac{1}{2}K_e(Q_\theta^2+Q_\epsilon^2)+V_aQ_a+A(Q_\theta^3-3Q_\theta Q_\epsilon^2)]\underline{1}_0+[(V_e+PQ_a)Q_\theta+N_e(Q_\epsilon^2-Q_\theta^2)]\underline{E}_\theta$$
$$+[(V_e+PQ_a)Q_\epsilon+2N_eQ_\epsilon Q_\theta]\underline{E}_\epsilon\ , \tag{2}$$

where $\underline{1}_0$ is the unit matrix, $\underline{\sigma}_x$ and $\underline{\sigma}_z$ are the Pauli matrices, and the $\underline{E}_\theta$ and $\underline{E}_\epsilon$ matrices are defined by (3),

$$\underline{E}_\theta=\frac{1}{2}\begin{bmatrix}1&0&0\\0&1&0\\0&0&-2\end{bmatrix},\quad \underline{E}_\epsilon=\frac{\sqrt{3}}{2}\begin{bmatrix}-1&0&0\\0&1&0\\0&0&0\end{bmatrix}. \tag{3}$$

The expansions (1) and (2) contain all linear and quadratic terms allowed by the symmetry. In addition, the anharmonic term cubic in e_g displacements (A) was also taken into account (because of its importance to the cooperative JT effect in $KCuF_3$ and K_2CuF_4).[7] Of course, the various JTC constants (V_e, N_e, and P), harmonic force constants (K_a and K_e), and anharmonic constants (A) are allowed to be different for the ^2E_g and $^2T_{2g}$ electronic states.

The calculations of the adiabatic potential constants for a_{1g} displacements provide values of the octahedral ligand field splitting parameter $10Dq=E(^2T_{2g})-E(^2E_g)$. We find $10Dq$ values of 6558, 6023, and 5540 cm^{-1} for Cu-F distances of 2.00, 2.03, and 2.06 Å, respectively. The CI contributions to these values are 20, 21, and 22%, respectively. The CT admixtures (i.e., the ratios of the CT and dominant d-shell configuration coefficients in the CI wave function) are -0.079 in the ^2E_g state and -0.040 in the $^2T_{2g}$ state. This is about half the size of CT admixtures for CuF_2,[11] but the CI contributions to the energy separations are of comparable importance.

The calculated JTC and harmonic force constants are given in Table IV. The effect of the CI is most important for the V_e, N_e, and P constants describing the JT splittings of the ^2E_g and $^2T_{2g}$ levels in the presence of the e_g-type fluorine distortion. The *ab initio* linear JTC constants $V_e(^2E_g)=-1.72\times10^{-9}$ N, $V_e(^2T_{2g})=0.60\times10^{-9}$ N are close to the results of the semiempirical calculations,[7] -1.82×10^{-9} N and 0.65×10^{-9} N, respectively. However, the quadratic constant N_e for the ^2E_g state differs greatly. We find $N_e(^2E_g)=-0.90$ N/m, whereas -6.33 N/m was obtained in Ref. 7. The P constants were not evaluated in the semiempirical calculations.[7]

As shown in the preceding section, the CI calculations provide energy separations between the Cu^{2+} levels in K_2CuF_4 with an accuracy of about 10%. Therefore, we suppose that the accuracy of the calculated $(CuF_6)^{4-}$ JTC constants (describing *splitting* of the ^2E_g and $^2T_{2g}$ states in

TABLE IV. The adiabatic potential constants for $(CuF_6)^{4-}$ based on the octahedral structure with $R=2.03$ Å.

	Potential-energy constants						
	Linear	Harmonic		Anharmonic	JT constants		
Term	V_a (10^{-9} N)	K_a (N/m)	K_e (N/m)	A (10^{11} N/m^2)	V_e (10^{-9} N)	N_e (N/m)	P (N/m)
^2E_g, HF	−7.78	192	83.5	−2.63	−1.45	−0.997	15.4
^2E_g, CI	−7.52	189	81.6	−2.65	−1.72	−0.901	17.4
$^2T_{2g}$, HF	−8.99	210	92.5	−2.52	0.51	1.42	−2.78
$^2T_{2g}$, CI	−8.90	208	89.3	−2.44	0.60	2.46	−4.17

the presence of e_g distortion) is also approximately 10%. No direct comparison can be made of the values calculated for K_a and K_e [for the free $(CuF_6)^{4-}$ cluster] with experimental data, but the reliability of our harmonic force constant calculations is indicated by the results for CuF_2. For the CuF_2 antisymmetric stretch, we obtain[11] a vibrational frequency of 761 cm^{-1}, in excellent agreement with the experimental value[14] of 769 cm^{-1} (the force constants are 404 and 413 N/m, respectively).

Figure 2 displays the $(CuF_6)^{4-}$ adiabatic potentials [i.e., eigenvalues of (1) and (2)] as functions of Q_θ for $Q_a=0$, $Q_\epsilon=0$. The anharmonicity term (A) and quadratic JT term (N_e) give rise to a significantly asymmetric adiabatic potential curve for the ground state, leading to a minimum corresponding to an elongated fluorine octahedron with $Q_\theta^{\min}=0.283$ Å and the JT stabilization energy of $E_{JT}=1075$ cm^{-1}. Neglecting the A and N_e terms in (1), one obtains for the ground state two equivalent minima at $Q_\theta^{\min}=\pm 0.210$ Å with $E_{JT}=V_e^2/2K_e=915$ cm^{-1}.

The negative sign of A leading to the *elongation* of the fluorine octahedron can be understood on the basis of simple qualitative considerations. The cubic anharmonic terms for bond stretch $[c(R-R_0)^3]$ generally have negative c since the bond must dissociate to a finite limit. For the Q_θ mode, these anharmonic terms necessarily favor $Q_\theta>0$ over $Q_\theta<0$ since the largest distortions (in the z axis) are positive for $Q_\theta>0$. More quantitatively, assuming that the $(CuF_6)^{4-}$ cluster elastic energy is a sum of $Cu^{2+}-F^-$ pair interaction potentials $[V_{Cu\text{-}F}=V_0+a(R-R_0)+b(R-R_0)^2+c(R-R_0)^3+\cdots]$, we obtain $A=c/2\sqrt{3}$; thus, A is negative.

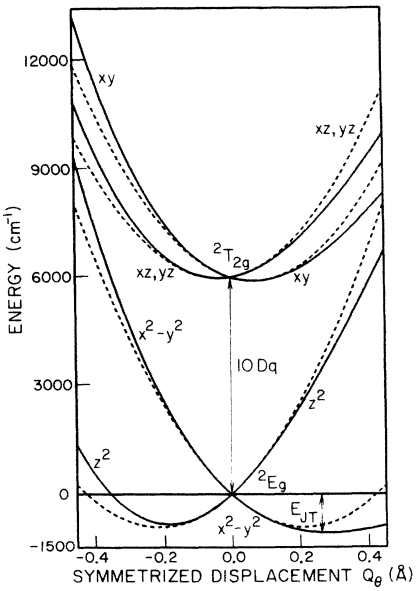

FIG. 2. Adiabatic potentials of $(CuF_6)^{4-}$ (CI results) as a function of Q_θ with $Q_a=0$ and $Q_\epsilon=0$. Here $10Dq=6023$ cm^{-1} and $E_{JT}=1075$ cm^{-1}. Solid lines: anharmonic and second-order JT terms are included; dotted lines: anharmonic and second-order JT terms are excluded.

For the excited state, the adiabatic potential minimum at $Q_\theta^{\min}=0.067$ Å corresponds also to elongation of the fluorine octahedron ($E_{JT}=98$ cm^{-1}). Neglect of A,N_e in (2) leads to the same $Q_\theta^{\min}$ and $E_{JT}=100$ cm^{-1}; therefore, the anharmonicity effects are insignificant for the excited state.

These JTC results are important for understanding the cooperative JT ordering in $KCuF_3$ and K_2CuF_4 crystals. Indeed, using a very simple theoretical model, Nikiforov *et al.*[7] showed that the type of cooperative JT ordering depends on the sign and the value of

$$g=A\rho^3-N_e\rho^2, \tag{4}$$

where $\rho=(Q_\theta^2+Q_\epsilon^2)^{1/2}$ is the magnitude of the JT distortion around each copper ion. The experimental crystal structures correspond to $g<0$, and the value $g=-160$ cm^{-1} was accepted in Ref. 7 (without calculation of A) to explain the observed ordering. The $KCuF_3$ experimental value of $\rho=0.382$ Å (Ref. 15) coupled with the parameters N_e and g used in Ref. 7 leads to $N_e\rho^2=-464$ cm^{-1} and $A\rho^3=-624$ cm^{-1}. Therefore, Ref. 7 assumed that the crystallographic ordering transformation (doubled unit cell) was determined by the competition of equally important contributions $N_e\rho^2$ and $A\rho^3$. The present calculations give $N_e\rho^2=-66$ cm^{-1} and $A\rho^3=-740$ cm^{-1} (for $\rho=0.382$ Å). Thus we conclude that the type of JT ordering observed in $KCuF_3$ and K_2CuF_4 crystals is caused by the anharmonicity contribution (rather than the second-order JT interaction). The calculated HF and CI energies of $(CuF_6)^{4-}$ for all geometries under consideration are given in the Appendix.

IV. CONCLUSIONS

The present *ab initio* calculations confirm the interpretation of the K_2CuF_4 optical-absorption spectrum suggested in Refs. 1, 4, and 8. The electron correlation (many-body) effects increase the d-d transition energies by about 20%, leading to good agreement with the experimental data.

We find considerable CI contributions to some of the JTC constants. The calculated values of the quadratic JTC and anharmonic constants for the ^2E_g state provide a new explanation of the microscopic mechanism leading to particular types of cooperative JT ordering in $KCuF_3$ and K_2CuF_4. Using the model suggested by Nikiforov *et al.*,[7] we find that the determining factor behind the distorted structures in these crystals is the anharmonicity of the Cu^{2+} ground-state adiabatic potential (the effect of quadratic JT term is negligible).

These results indicate that rather simple CI calculations on transition-metal cluster systems can lead to valuable contributions to the understanding of the ligand field and Jahn-Teller splittings in bulk systems.

ACKNOWLEDGMENTS

This work was partially supported by the U.S. Office of Naval Research (Contract No. N00014-84-K-0637). We

wish to thank Mark Brusich for his help in computer calculations. We also thank the International Research and Exchanges Board for helping to arrange the sojourn of one of the authors (S.Y.S.) at the California Institute of Technology.

APPENDIX

The a_{1g} and e_g distortions of the $(CuF_6)^{4-}$ cluster are displayed in Fig. 3. The coordinates of these displacements are defined as follows:

$$Q_a=(X_1-X_4+Y_2-Y_5+Z_3-Z_6)/\sqrt{6}\ ,$$
$$Q_\theta=(2Z_3-2Z_6-X_1+X_4-Y_2+Y_5)/\sqrt{12}\ , \quad (5)$$
$$Q_\epsilon=(X_1-X_4-Y_2+Y_5)/2\ ,$$

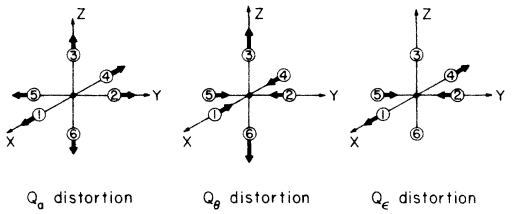

FIG. 3. The symmetrized displacements of an octahedral cluster.

where $X_i=x_i-x_i^0$, $Y_i=y_i-y_i^0$, and $Z_i=z_i-z_i^0$ are the displacements of the ith F^- ion.

Tables I and II present the calculated HF and CI energies (AC approximation) for all distorted $(CuF_6)^{4-}$ configurations considered in obtaining the adiabatic potential constants.

*Permanent address: Physics Department, A. M. Gorkii Ural State University, Sverdlovsk, 620083, U.S.S.R.

[1]D. I. Khomskii and K. I. Kugel, Solid State Commun. **13**, 763 (1973).
[2]R. Haegele and D. Babel, Z. Anorg. Allg. Chem. **409**, 11 (1974).
[3]W. Kleeman and Y. Farge, J. Phys. (Paris) **36**, 1293 (1975).
[4]R. Laiho, Phys. Status Solidi B **69**, 579 (1975).
[5]J. Ferre, M. Regis, Y. Farge, and W. Kleemann, J. Phys. C **12**, 2671 (1979).
[6]J. Kanamori, J. Appl. Phys. **31**, 145 (1960).
[7]A. E. Nikiforov, S. Yu. Shashkin, M. L. Levitan, and T. H. Agamalyan, Phys. Status Solidi B **118**, 419 (1983).
[8]S. Yu. Shashkin and A. E. Nikiforov, Fiz. Tverd. Tela (Leningrad) **25**, 84 (1983).
[9]S. Larsson, B. O. Roos, and P. E. M. Siegbahn, Chem. Phys. Lett. **96**, 436 (1983).
[10]T.-K. Ha and M. T. Nguyen, Z. Naturforsch. Teil A **39**, 175 (1984).
[11]S. Yu. Shashkin and W. A. Goddard III, J. Phys. Chem. (unpublished).
[12]A. J. H. Wachters and W. C. Nieuwpoort, Phys. Rev. B **5**, 4291 (1972).
[13]F. W. Bobrowicz and W. A. Goddard III, in *Methods of Electronic Structure Theory* (Plenum, New York, 1977), p. 79.
[14]P. H. Kasai, E. B. Whipple, and W. Weltner, J. Chem. Phys. **44**, 2581 (1966).
[15]A. Okazaki and Y. Suemune, J. Phys. Soc. Jpn. **16**, 176 (1961); A. Okazaki, *ibid.* **26**, 870 (1969).